Biological Psychology 36 (1993) 3–21

Signal fidelity requirements for deriving impedance cardiographic measures of cardiac function over a broad heart rate range

Barry E. Hurwitz, Liang-Yu Shyu, Chih-Cheng Lu, Sridhar P. Reddy, Neil Schneiderman and Joachim H. Nagel

Behavioral Medicine Research Center, Departments of Psychology, Medicine and Biomedical Engineering, University of Miami, FL, USA

Our findings indicate that the impedance cardiogram spectrum extends from DC to 50 Hz. Any amplifier with an upper band limit less than 50 Hz can be expected to produce attenuation and distortion of the impedance cardiogram. This signal attenuation may be systematically enhanced under conditions of high heart rate when a greater proportion of signal energy will be in the upper frequency range of the impedance cardiogram spectrum. Therefore, the present study was designed to assess the influence of amplifier bandwidth on dZ/dt_{max}, stroke volume, and systolic time intervals (LVET, PEP, QZ, QX). Simultaneously measured ΔZ and dZ/dt signals from two impedance cardiographs, with corner frequencies of 120 and 60 Hz for the ΔZ and 50 and 15 Hz for dZ/dt channels, were contrasted over a broad range of heart rate (70–150 bpm). In addition to the analog dZ/dt signals obtained from the instruments, the ΔZ signals were digitally converted to dZ/dt by off-line digital differentiation with a 50 Hz corner frequency. The results demonstrated that the measurements with the 15 Hz corner frequency, when compared with the 50 Hz corner frequency measurements, systematically attenuated the dZ/dt_{max} amplitude and stroke volume measurements as heart rate increased. The attenuation of dZ/dt_{max} and stroke volume ranged from about 13% to 26% as heart rate increased from 70 to 150 bpm. When the upper bandlimit was 50 Hz, the dZ/dt signal had greater resolution of waveform events and produced less prolonged systolic time intervals. The 15 Hz amplifier differentially influenced the B point, Z-peak and X minimum, having no apparent effect on the temporal location of the B point, but delaying the Z-peak about 21.7 ms and the X minimum about 7.4 ms. These findings indicate that impedance cardiographs with insufficient upper bandlimits will differentially influence ICG-derived measurements as heart rate varies.

Keywords: impedance cardiography, signal fidelity, instrumentation, spectrum, stroke volume, systolic time intervals, exercise

Correspondence to: Barry E. Hurwitz, Ph.D., Behavioral Medicine Research Center, Department of Psychology, University of Miami, P.O. Box 248185, Coral Gables, FL 33124, USA

Introduction

Impedance cardiography is a noninvasive, atraumatic, and relatively unobtrusive technique, which has been used for more than two decades to provide a continuous measure of beat-by-beat change in stroke volume (SV) (Geddes & Baker, 1989; Miller & Horvath, 1978). In addition to SV, cardiac output, systolic time intervals and several related cardiovascular parameters may be obtained. Thus when using this technique a comprehensive cardiovascular functional analysis may be performed in the resting and behaving human. Although impedance cardiography has achieved increasing popularity as a research tool (Sherwood et al., 1990), it has not yet found adequate application as a clinical diagnostic tool (Fuller, Raskob, Ter Keurs & Hull, 1989). Validity studies comparing impedance cardiography-derived SV or cardiac output values with various gold standards have not always shown absolute agreement, although, in general, high correlations are obtained if group data are considered (see review of Geddes & Baker, 1989). The single subject data, however, even from studies showing excellent overall validity indicate that the error between the different techniques can exceed 30% even for healthy subjects (e.g. Appel, Kram, MacKabee, Fleming & Shoemaker, 1986; Bernstein, 1986).

Fewer validity studies have been performed during dynamic cardiovascular challenge than during stable-state resting conditions. One study, for example, which compared impedance cardiography with thermodilution estimates of cardiac output during conditions of cardiac pacing and pharmacologic challenge observed relatively high correlations (Goldstein, Cannon, Zimlichman & Keiser, 1986). In contrast, in a more recent study, which compared impedance cardiography with nuclear ventriculography estimates of SV at rest and during exercise, high correlations at rest were observed but progressively declining correlations were found with higher exercise workloads (Wilson, Sung, Pincomb & Lovallo, 1989). Findings such as these have led others, as in a recent U.S. Health and Human Services report (Handelsman, 1989), to conclude that impedance cardiography should not be considered a valid tool for diagnostic purposes in single patients with abnormal cardiovascular function, such as in those with rapid heart rates (HR) or during dynamic challenge conditions such as exercise. The conclusion that impedance cardiography lacks validity may be somewhat unjustified, since discrepant impedance cardiography-derived values may be a consequence of methodological shortcomings of the reported studies rather than insufficiencies in the theoretical underpinnings of impedance cardiography. For example, in individuals displaying faster HRs at rest or under exercise conditions, impedance cardiogram (ICG) attenuation may be systematically influenced by the fidelity of the amplifier, especially during higher HRs when a greater proportion of signal energy is in the higher frequency portion of the ICG

spectrum. Thus the fidelity of the front-end instrumentation may influence the validity of impedance cardiography.

Spectrum of the impedance cardiogram

To establish the appropriate signal fidelity requirements for the impedance cardiographic instrumentation, it is first necessary to determine the ICG spectrum, which to our knowledge has not previously been documented. To do this, an impedance cardiograph with a 2 mA, 100 kHz constant current source and a wideband 265 Hz anti-aliasing filter at the amplifier output was used to collect an ICG signal (ΔZ). The ICG spectra of ten continuous cardiac cycles at low (70–89 bpm) and high (130–149 bpm) HRs were obtained from seven subjects with a spectral resolution of 0.98 Hz. The spectra were then averaged across the subjects at both HR levels (see Fig. 1). The purpose of this spectral analysis was to specify the bandwidth, noise and dynamic range necessary for an ICG amplifier to provide optimum performance for subsequent event detection and amplitude measurement. Therefore, the upper bandlimit of the ICG may be defined as the frequency where the signal power drops below the power of the noise. In the ICG spectrum the "white" system noise component can clearly be identified as the spectrum baseline. When the system noise is subtracted from the average spectrum, the spectrum due to signal remains (see Fig. 1). An upper band limit derived from this average spectrum will represent the ICG of the majority of subjects. However, individuals with more uncharacteristic elements within the ICG waveforms will not be represented nor will the inherent variation of the ICG signal within individuals be accounted for. Previous solutions to the problem of establishing an upper bandlimit are

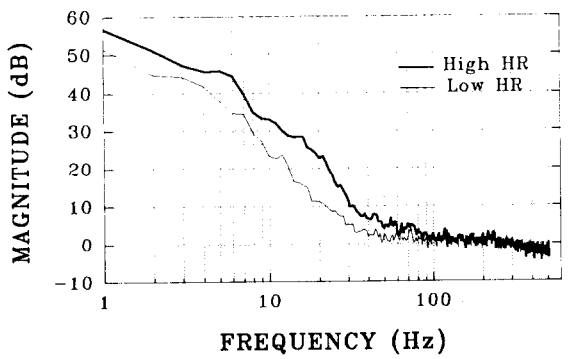

Fig. 1. Averaged spectra of ΔZ at low (70–89 bpm) and high (130–149 bpm) heart rate (HR) after the spectrum of the system noise is removed.

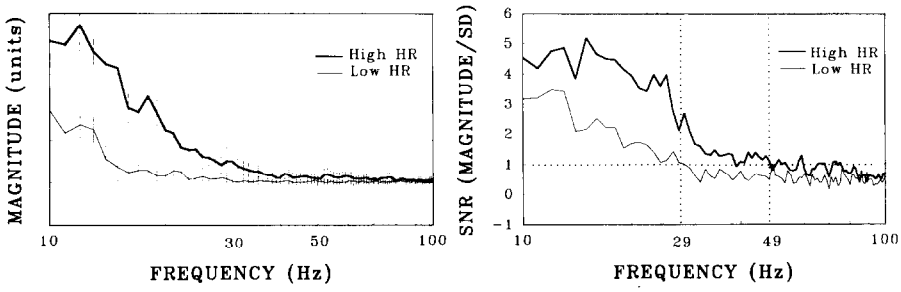

Fig. 2. Depicted in the left panel at low heart rate (HR) (70–89 bpm, thin line) and high HR (130–149 bpm, thick line) is the mean ± SD ICG spectrum from a representative subject. In the right panel the signal-to-noise ratio (SNR) of the ΔZ spectrum averaged across all subjects is shown. In the right panel upper bandlimits are denoted where the vertical lines cross the horizontal line, which is the frequency at which the SNR is one.

based on the measurement of spectral averages. The determined upper bandlimit may be adequate on average but this procedure does not provide optimal representation of the largest percentage of total spectral power over the widest range of individual variation.

An alternative may be found when considering the relationship of the average spectrum to its variance. Figure 2 (left panel) displays the intraindividual variation (mean ± SD) of the ICG spectrum of a representative subject. Since detection algorithms are generally based on the typical appearance of these signals, intra- or interindividual variance of signal shape may be considered as a measure of the "physiological noise". Thus the ICG bandwidth may be determined by calculating the average spectra, subtracting the baseline system noise and deriving the physiological signal-to-noise ratio. The signal-to-noise ratio for a given frequency was calculated as the ratio of average power and its standard deviation (see Fig. 2, right panel). Then the upper bandlimit was determined by locating the frequency where the signal-to-noise ratio declines below one. This procedure limits the spectral band of the signal to those frequencies where the contribution of the true signal is larger than that of physiological noise and interferences. Inspection of Fig. 2 (right panel) reveals that the ICG spectrum ranges within 30 Hz at slower HR levels and increases to 50 Hz at faster HR levels, when the signal-to-noise ratio equals one.

In general, the bandwidth of most of the commercially available impedance cardiographs appears to be insufficient to produce the ICG-dZ/dt without attenuation or distortion. Since the Minnesota impedance cardiograph model 304B (MIC) is the most widely used impedance cardiograph, we have selected it to use in this study. A frequency response analysis of the MIC [1] showed upper band limits of 60 Hz for the ΔZ channel and 15 Hz for the dZ/dt channel. Since the ICG spectrum extends to 50 Hz, at the very least

ICG systems with corner frequencies less than 50 Hz would be expected to attenuate the signals under conditions of high HRs when a greater proportion of signal energy is in the higher frequency range of the ICG spectrum. Therefore, to examine the influence of signal fidelity, the ICG values derived from the MIC were compared with values derived from an impedance cardiograph (UM) developed in our laboratory. A frequency response analysis of the UM impedance cardiograph revealed an upper band limit of 120 Hz for ΔZ and 50 Hz for dZ/dt. Therefore, since an HR-dependent outcome was anticipated, the primary interest of this study was to examine the influence of signal fidelity on ICG-derived dZ/dt_{max}, SV and systolic time interval indices over a broad range of HR (70–150 bpm). Specifically, simultaneously measured ΔZ and dZ/dt signals from two impedance cardiographs with corner frequencies of 120 and 60 Hz for the ΔZ and 50 and 15 Hz for dZ/dt channels were contrasted. In addition, the ΔZ signals were converted to dZ/dt by off-line digital differentiation with a 50 Hz corner frequency. Thus the cardiac parameters derived from the analog dZ/dt signal using an amplifier with a 15 Hz corner frequency (MIC-15 Hz) were compared with the cardiac parameters derived using three amplifiers all of which used a 50 Hz corner frequency. They were the analog dZ/dt signal amplifier (UM-50 Hz) and the two digitally computed dZ/dt signal amplifiers (MIC-60 Hz and UM-120 Hz). The purpose of using the two digital differentiators was to investigate the influence of the differentiator quality on signal fidelity. The performance of digital differentiators comes much closer to an ideal differentiator than the low order analog differentiators normally used in impedance cardiographs. Physiological measurements were obtained during rest and during a bicycle exercise procedure in which the workload was adjusted to induce HRs in the following bpm ranges: 70–89, 90–109, 110–129 and 130–149.

Balancing the impedance cardiogram signal

An additional instrumentation issue, which may impact on the validity of the ICG, pertains to electronic techniques for balancing the ΔZ signal.

[1] It should be noted that the frequency response analysis was performed on two model 304B, MICs with identical findings. A schematic circuit diagram of the MIC (dated September 27, 1985) indicates that, although the ΔZ and dZ/dt circuits are shown to have corner frequencies of 97 Hz and 68 Hz, respectively, the signal passes through three previous stages with low pass filters at each stage. The combined effect of these filters, as determined by computer simulation, is to reduce the corner frequencies to 88 Hz and 40 Hz, respectively. Therefore, the difference between the corner frequencies derived from computer simulations of the schematic and that actually measured from the model 304B suggests that earlier MIC models may have larger bandwidths than that used in the model 304B.

Typically, movement produces a large amount of change in mean thoracic impedance (Z_0) relative to the changes in the ΔZ signal. These changes in Z_0 require balancing adjustment to enable changes in ΔZ to be measured within the limited dynamic range of the amplifier. Kubicek, Karnegis, Patterson and From (1974) developed a sample and hold balancing circuit, which is presently used in the MIC. This circuit operates by abruptly shifting the signal baseline whenever the ΔZ output drifts outside the active range of the amplifier. Thus the signal is maintained within the channel but a discontinuity in the signal is introduced when resampling begins, producing an artifact in the ΔZ. Others have attempted modifications of the sample and hold circuit, with some improvement, but the sample and hold function remains leaving the signal susceptible to artifactual influences and data loss, especially when the ICG is measured during procedures requiring movement, such as exercise (Anderson, Cobbold & Johnston, 1981). In the UM impedance cardiograph used in the present study, a real-time automatic balancing circuit was used (Lu, 1991). This circuit continuously removes the baseline shift by measuring the trend in the signal using a low-pass filter and subtracting this trend from the original signal. The ΔZ signal is thus maintained within the active range of the amplifier without producing signal discontinuities. Figure 3 depicts the ΔZ and dZ/dt, which was digitally computed from the ΔZ measured from two subjects. The artifact inducing action of the sample and hold circuit on the dZ/dt signal (left panel) can be contrasted with the action of the automatic balancing circuit on a simultaneously measured ICG signal (right panel). Therefore, a secondary interest of the present study was to compare the functioning of the sample and hold and automatic-balancing circuits, while subjects were at rest and while bicycle exercising at HRs of 110–129, and 130–149 bpm.

Method

Subjects

Ten healthy men reporting no cardiopulmonary or other medical disorders, aged between 21 and 45 years (mean 29.9 ± 7 years), served as subjects. The subjects' respective mean ± SE body weight, height and body surface area were 69.4 ± 3 kg, 176.0 ± 2 cm, and 1.85 ± 0.1 m^2.

Apparatus

During the testing session an electrocardiogram (ECG) and phonocardiogram (PCG) were recorded using Grass polygraph amplifiers. A standard lead II ECG configuration was used. The PCG was recorded by placing the

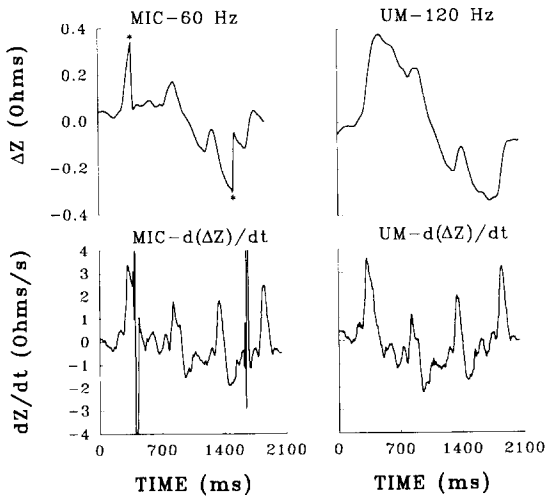

Fig. 3. The ΔZ simultaneously sampled from an individual exercising subject for four cardiac cycles using the MIC-60 Hz (left panel) and UM-120 Hz (right panel) instruments. The MIC sample and hold balancing circuit function is contrasted with the real-time automatic balancing circuit of the UM machine. Where the signal exceeds the channel barrier at about ± 0.4 Ω, the MIC balancing circuit on two occasions (see * in left-top panel) instantly shifted the ΔZ signal to the channel centerline producing spike artifacts when the dZ/dt is computed by digital differentiation (see left-bottom panel). No such ΔZ signal corrections (see right-top panel) or artifacts (see right-bottom panel) were produced by the UM balancing circuit.

phonotransducer (Hewlett Packard 21050A) on the cardiac window in the second intercostal space just left of the sternum. This measure provided confirmation of the location of the ICG-X wave reflecting aortic valve closure. The ICG signals—ΔZ, dZ/dt and Z_0—were simultaneously recorded using the MIC (model 304B) and UM impedance cardiographs. The ICG was derived using a tetrapolar electrode configuration, with bands placed 360° around the body (Hurwitz, Shyu, Reddy, Schneiderman & Nagel, 1990), where a 4 mA, 100 kHz constant current from the UM impedance cardiograph was applied to the thorax through the first and fourth ICG leads. The ICG was simultaneously transmitted to both impedance cardiographs via the second and third ICG leads. The mean of the front and back distance between ICG leads 2 and 3 was measured for later use in calculation of SV using the Kubicek equation (Kubicek, Witsoe, Patterson & From, 1969). All signals were sampled in discrete 30 s samples by an IBM PS/2 model 70 computer at 1 kHz sampling rate using an A/D converter (DT 2901). Impedance calibration signals for the three ICG signals were also stored in the computer for later conversion of the ICG measurements to the corresponding units.

Procedure

While subjects were seated on an exercise bicycle (Tunturi), physiological measurements were obtained at rest and during an exercise procedure in which the cycling workload was adjusted to produce HRs in the following bpm ranges: 70–89, 90–109, 110–129, and 130–149. At each of the four target HR ranges a sample was collected. The resting sample (i.e. 70–89 bpm) was taken while the subjects were seated but not pedaling the bicycle. For the other three sample collections, when the experimenter determined that the subjects' HR was within the target ranges, subjects were instructed to stop cycling. To permit comparison of the sample and hold and real-time automatic-balancing circuits during exercise, two additional samples were taken when the subjects were cycling, i.e. when the subjects' HR was in each of the two fastest target ranges. More detailed information about the real time automatic-balancing circuitry has been previously presented (Lu, 1991).

Data quantification

The parameters were derived from ensemble averages in which the ECG, PCG and dZ/dt analog signals from 15 consecutive cardiac cycles were averaged on a beat-by-beat basis temporally synchronized with the R-wave of the ECG. The 15 consecutive cycles were selected from the 30 s samples taken within each of four HR ranges. A computed dZ/dt was also used, wherein the derivative of the measured ΔZ was calculated using a nonrecursive digital differentiator, with a corner frequency of 50 Hz, transition bandwidth of 5 Hz and minimum stopband rejection of -20 dB.

For the digitally computed dZ/dt, signal parameters were derived from ensemble averages of the identical 15 consecutive cycles used in the ensemble averages of the analog dZ/dt signal. ICG events were located automatically and the displayed event markers could be manually adjusted. The dZ/dt_{max} was defined as the amplitude difference between the B-point and the maximum of the dZ/dt. Left ventricular ejection time (LVET) was determined as the interval between the B point and the X minimum. The mean Z_0 during systole averaged across the 15 cardiac cycles and the blood resistivity constant of 135 Ω cm were used in the Kubicek equation. Systolic time intervals such as pre-ejection period (PEP—measured from Q onset to B), time to maximal ejection velocity (QZ), as well as the electromechanical systole (QX), were also measured. Therefore, the present study examined: (a) the influence of signal fidelity for the analog dZ/dt signals (MIC-15 Hz vs. UM-50 Hz) and for the digitally computed dZ/dt signals (MIC-60 Hz vs. UM-120 Hz) on measurement of cardiovascular functioning over a broad range of HR; and (b) the performance of the balancing circuits (sample and hold vs. automatic balancing) at rest and during two levels of bicycle exercise.

Results

The primary data analyses to examine the influence of signal fidelity across the four HR intervals used repeated measures analyses of variance to compare the cardiovascular parameters (dZ/dt_{max}, SV, LVET, PEP, QZ and QX) derived from the four measurement methods: MIC-15 Hz, UM-50 Hz, MIC-60 Hz, and UM-120 Hz. The secondary analyses to examine the effect of the two electronic methods of ΔZ balancing on ICG artifact induction used repeated measures analyses of variance to compare the balancing methods during bicycle exercise across the three periods: rest (70–89 bpm), exercise 1 (110–129 bpm) and exercise 2 (130–149 bpm).

The influence of signal fidelity on ICG-derived values

The bicycle exercise procedure produced four significantly distinct HR levels within the four target ranges ($F(3,27) = 345.0$, $p < 0.001$), with mean ± SD bpm values of 74.6 ± 5.3, 100.2 ± 6.0, 119.8 ± 6.6 and 139.7 ± 7.6. Figure 4 depicts the mean dZ/dt_{max} and SV digitally computed from the derivative of ΔZ (MIC-60 Hz vs. UM-120) and measured from the analog dZ/dt signal (MIC-15 Hz vs. UM-50 Hz) during the four HR intervals. Differences were revealed for dZ/dt_{max} over the HR ranges (Figure 4, top panel); the computed UM-120 Hz value was significantly greater than the computed MIC-60 Hz value ($F(1,9) = 6.4$, $p < 0.05$) and the analog UM-50 Hz value ($F(1,9) = 195.4$, $p < 0.001$). No differences were found between the last two signal bandwidths (MIC-60 Hz, UM-50 Hz) but these values were significantly greater than the analog MIC-15 Hz value ($F(1,9) = 57.4$, $p < 0.001$; $F(1,9) = 165.0$, $p < 0.001$, respectively). Mean ± SD dZ/dt_{max} Ω s^{-1} values for UM-120 Hz, MIC-60 Hz, UM-50 Hz and MIC-15 Hz were 2.92 ± 0.5, 2.76 ± 0.4, 2.73 ± 0.4, 2.19 ± 0.4, respectively.

Similar differences were observed for SV over the HR ranges (Fig. 4, bottom panel); the computed UM-120 Hz value was significantly greater than the computed MIC-60 Hz value ($F(1,9) = 14.3$, $p < 0.005$) and the analog UM-50 Hz value ($F(1,9) = 154.2$, $p < 0.001$). No differences were found between the last two signal bandwidths (MIC-60 Hz, UM-50 Hz) but these values were significantly greater than the analog MIC-15 Hz value ($F(1,9) = 56.9$, $p < 0.001$; $F(1,9) = 148.5$, $p < 0.001$, respectively). Mean ± SD SV ml values for UM-120 Hz, MIC-60 Hz, UM-50 Hz and MIC-15 Hz were 75.1 ± 15, 70.0 ± 13, 69.8 ± 14, 57.8 ± 12, respectively.

In addition to differences between the four measurement methods in overall level of dZ/dt_{max} and SV, the attenuation in the MIC-15 Hz analog dZ/dt signal becomes more severe with increasing HR (see Fig. 4). For example, when the UM-50 Hz dZ/dt_{max} values were compared with the MIC-15 Hz dZ/dt_{max} values a significant interaction was found between

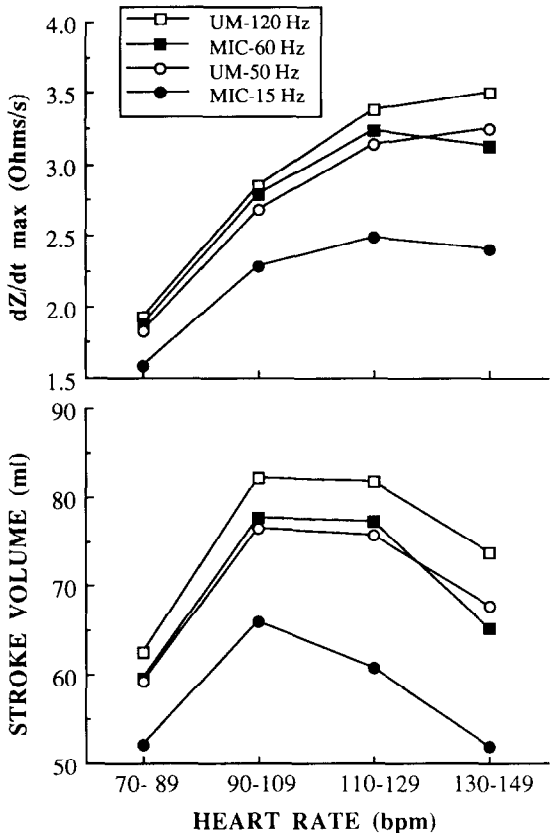

Fig. 4. This figure displays the mean dZ/dt_{max} (top panel) and stroke volume (bottom panel) values over the four target heart rate ranges produced by the four measurement methods.

measurement method and a linear trend of increasing dZ/dt_{max} values over the HR periods ($F(1,9) = 17.9$, $p < 0.001$); percentage differences in dZ/dt_{max} and SV values increased from about 13% at the slowest HR period to 26% at the fastest HR period. Therefore, greatest attenuation of dZ/dt_{max} and SV is present when these parameters are derived from the analog dZ/dt signal of the MIC instrument with the 15 Hz corner frequency, which produced progressively greater attenuation with increasing HR. Figure 5 displays, in a representative subject, greater dZ/dt_{max} obtained using the UM-120 Hz corner frequency (thick line) than measured using the MIC-15 Hz corner frequency (thin line); this difference appears to be present at both low (84 bpm) and high (141 bpm) HRs. Note the greater resolution of the relevant signal events (B point, dZ/dt peak and X wave) in the UM-120 Hz dZ/dt ensemble averages.

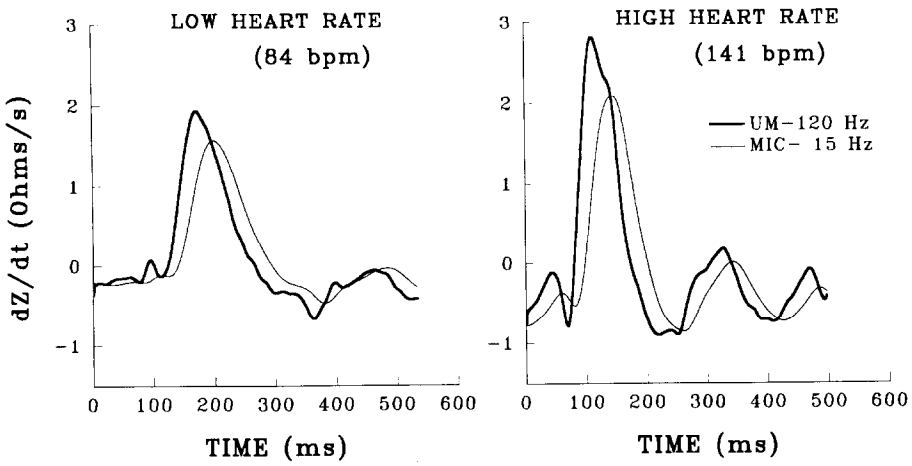

Fig. 5. Ensemble averages from a representative subject depict greater dZ/dt_{max} obtained using the UM-120 Hz corner frequency (thick line) than measured using the MIC-15 Hz corner frequency (thin line) at rest (84 bpm) and following high exercise workload (141 bpm). Greater resolution of the relevant waveform events (B point, dZ/dt peak and X wave) in the UM-120 Hz dZ/dt ensemble averages can be seen at both heart rate levels.

Table 1 depicts the effect of the four measurement methods on the systolic time intervals: LVET (BX), PEP (QB), QZ, and QX. For LVET there was no significant difference between three methods (UM-120 Hz, UM-50 Hz, MIC-60 Hz) across the HR levels. However, the MIC-15 Hz method resulted in significantly more prolonged LVET than the other three methods, UM-120 Hz, UM-50 Hz, and MIC-60 Hz ($F(1,9) = 295.5$, $p < 0.0001$; $F(1,9) = 154.7$, $p < 0.0001$, $F(1,9) = 582.6$, $p < 0.0001$, respectively). Inspection of the means in Table 1 reveals about a 6.3 ms mean increase in the LVET measured using the analog MIC-15 Hz.

To address the question of whether the analog and computed methods have differing influences on the locations of the relevant events within the ICG (i.e. B point, Z peak, and X minimum) the following analyses separately examined the PEP, which is the QB interval, as well as the QZ and QX intervals. For PEP the two computed methods (UM-120 Hz and MIC-60 Hz) did not significantly differ. The two analog methods (UM-50 Hz and MIC-15 Hz) did not significantly differ either. However, the two analog methods produced more prolonged PEP by about 9.4 ms on average than the two computed methods (e.g. for UM-50 Hz vs. MIC-60 Hz, $F(1,9) = 62.8$, $p < 0.0001$). For the QZ interval the analyses revealed that the two computed methods (UM-120 Hz and MIC-60 Hz) did not significantly differ. The UM-50 Hz method, however, produced a significantly more prolonged QZ interval by about 8.9 ms on average than the two computed methods (for

Table 1

Mean (±SD) systolic time intervals comparing the measurement methods over the heart rate ranges

Parameter	Method	Heart rate range (bpm)			
		70–89	90–109	110–129	130–149
LVET (BX)	UM-120 Hz	269.2±23	238.7±13	201.4±12	176.8± 8
(ms)	MIC-60 Hz	268.5±22	236.5±10	203.6±12	178.7±11
	UM-50 Hz	268.8±22	236.7±13	200.8±12	175.6± 8
	MIC-15 Hz [a]	274.9±22	245.8±13	206.9±11	184.0±11
PEP (QB)	UM-120 Hz	96.0±17	66.3± 6	62.9± 8	61.3± 8
(ms)	MIC-60 Hz	96.3±16	67.1± 7	63.9±10	63.3±11
	UM-50 Hz [b]	105.5±17	75.1± 6	71.9± 7	71.1± 8
	MIC-15 Hz [b]	106.1±13	73.9±10	75.1±14	73.6±13
QZ	UM-120 Hz	168.1±14	122.0±15	105.4±15	98.9±15
(ms)	MIC-60 Hz	169.0±15	120.7±14	107.6±18	102.6±17
	UM-50 Hz [a]	177.8±14	131.4±15	115.4±15	108.2±14
	MIC-15 Hz [d]	197.4±15	150.4±11	139.5±17	132.0±16
QX	UM-120 Hz	365.2±16	305.0±16	264.3±13	238.1±10
(ms)	MIC-60 Hz	364.8±15	303.6±13	267.5±18	242.0±17
	UM-50 Hz [c]	374.3±16	311.8±16	272.7±13	246.7±11
	MIC-15 Hz [d]	381.0±17	319.7±14	282.0±18	257.6±17

[a] $p < 0.0005$ (MIC-15 Hz significantly longer than all other methods across HR levels).
[b] $p < 0.0001$ (Both UM-50 Hz and MIC-15 Hz significantly longer than other two methods across HR levels).
[c] $p < 0.0001$ (UM-50 Hz significantly longer than MIC-60 Hz and UM-120 Hz across HR levels).
[d] $p < 0.0001$ (MIC-15 Hz significantly longer than UM-50 Hz across HR levels).

UM-120 Hz $F(1,9) = 3645.9$, $p < 0.0001$; for MIC-60 Hz $F(1,9) = 71.0$, $p < 0.0001$). The MIC-15 Hz analog method resulted in an even more prolonged QZ than the UM-50 Hz analog method ($F(1,9) = 154.7$, $p < 0.0001$), with an average cumulative difference between the MIC-15 Hz method and the computed methods of about 30.6 ms. For the QX interval, similar to the QZ analyses, the two computed methods did not significantly differ. The UM-50 Hz method resulted in more prolonged QX intervals by about 8.9 ms on average relative to the computed methods (for UM-120 Hz $F(1,9) = 193.7$, $p < 0.0001$; for MIC-60 Hz $F(1,9) = 34.4$, $p < 0.0005$). The MIC-15 Hz method yielded significantly more prolonged QX than the UM-50 Hz ($F(1,9) = 44.2$, $p < 0.0001$), with an average cumulative difference between the MIC-15 Hz method and the computed methods of about 16.3 ms.

Therefore, in general, the analog methods produced more prolonged systolic time intervals than the digital methods. The UM-50 Hz analog method appeared to produce a consistent lengthening of the intervals of about 8–9 ms, with a similar delay in location for each of the three events B,

Table 2
ΔZ Balancing: Percentage ($\pm$SD) of cardiac cycles distorted using real-time auto-balancing (A-B) compared with sample and hold (S&H) functions

Rest (80 bpm)		Exercise 1 (110–129 bpm) [a]		Exercise 2 (130–149 bpm) [a]	
A-B	S&H	A-B	S&H	A-B	S&H
0.0 $\pm$	4.1 $\pm$ 10	0.0 $\pm$ 0	31.3 $\pm$ 25	0.0 $\pm$ 0	34.3 $\pm$ 22

[a] $p < 0.0001$ (A-B vs. S&H).

Z-peak and X. However, the MIC-15 Hz analog method produced an even greater delay in the Z-peak and X-minimum event locations relative to the other methods. Moreover, the MIC-15 Hz method appeared to differentially influence the ICG such that there was greatest prolongation in the QZ interval with less prolongation in the QX interval, which was more prolonged than the QB interval.

Comparison of two ΔZ balancing methods

The performance of the balancing circuits (sample and hold vs. real-time auto-balancing) was evaluated by measuring the percentage of cardiac cycles distorted by artifact at rest (70–89 bpm) and when HR was titrated up to two levels (110–129 and 130–149 bpm) during bicycle exercise. Table 2 depicts these findings. Analysis comparing the two balancing methods over the three HR ranges revealed a significant interaction between these effects ($F(2,18) = 27.2$, $p < 0.0001$). Follow-up comparisons were performed at each HR level. Although no difference between the two balancing methods was found at rest, significant differences were observed during both the first and second exercise levels (respectively $F(1,9) = 44.2$, $p < 0.0001$; $F(1,9) = 44.2$, $p < 0.0001$). Inspection of Table 2 indicates that the sample and hold balancing circuit produces ΔZ artifacts during exercise, which influences over 30% of the cardiac cycles; whereas the real time auto-balancing circuit produces a ΔZ signal that is free of the gross artifacts that completely distort the signal.

Discussion

To derive valid measures of cardiovascular function using impedance cardiography it is of primary importance that the instrumentation yield truly representative physiological waveforms. Therefore, the primary objective of the present study was to determine the amplifier specifications necessary to produce an ICG, with the highest possible signal fidelity and signal-to-noise ratio, with minimal signal delay. To achieve these goals the upper bandlimit

of the low pass filter of the front-end instrument must be set in correspondence with the ICG spectrum. The problem inherent in this process is that the ICG spectrum changes with the rate at which the heart beats. Therefore, the ICG spectrum was determined in the present study for the resting level (i.e. 70–89 bpm) and moderately high HRs (i.e. 130–149 bpm). Using the physiological signal-to-noise ratio method the upper band limit of the ΔZ signal was determined to be within 30 Hz at the lower HR range and within 50 Hz at the higher HR range. Therefore, an ICG amplifier that uses a low-pass filter with a 50 Hz corner frequency should maximize signal fidelity when HR is below 150 bpm.

The signal-to-noise ratio criterion used in this study to determine the upper bandlimit is novel and has been previously compared with more common practises in electrical engineering (Shyu, 1992). In summary, the two more commonly used methods to assess spectral bandwidth are the linear regression and percentage of total power methods. When linear regression lines are estimated for both baseline and signal segments of the ICG spectrum using the least mean square error criterion, with the intersection defining the band limit, the selection of the spectra segment to regress is problematic because the signal portion of the spectra is not linear at the lower frequencies (see Fig. 1). Thus the upper band limits were 50 and 70 Hz for high HRs depending upon whether the spectra considered were 1–100 Hz or 5–30 Hz, respectively. For low HRs the limits were 35 and 45 Hz when respective spectra for 1–50 Hz and 3–20 Hz were used in the linear regression estimations. Therefore, the lack of a clear procedure for selecting the appropriate spectrum bandwidth upon which linear regression is performed raises doubt as to which of these possible bandwidths is correct. The other commonly used method defines the upper bandlimit as the frequency below which the percentage of total power is 99.95%. For the ICG spectra in this study this corresponds to 16 and 21 Hz for low and high HRs, respectively. The criterion percentage of 99.95 is arbitrary and inspection of the ICG spectra (see Fig. 1) clearly shows that there are spectral components related to signal above these limits.

The signal-to-noise ratio method of calculating the ratio between the mean magnitude and its standard deviation at each frequency was used in this study instead of these methods. This method maintains the advantage of deriving the bandwidth from an averaged spectrum as the other methods do but also takes into account the variations of individual spectra reflecting individual differences in waveform topography. The criterion in which the upper bandlimit is determined as the frequency at which the signal-to-noise ratio drops to one permits an unbiased decision to be made in bandlimit selection. The results indicate that this method includes all the visible elevations above the spectral baseline, accounting for more than 99.99% of the total power, and yields an unbiased estimate of the ΔZ bandwidth.

Inspection of Fig. 1 reveals that the spectral components of the ICG at high frequencies on average contribute little to the power of the signal. However, these components may be significant in individual signals and may influence the amplitude, shape and temporal location of the events within the signal. Therefore, to assess the influence of signal fidelity on the measures of cardiac function derived from simultaneously measured dZ/dt and ΔZ signals, the present study compared the performance of two ICG instruments with different upper bandlimits over a broad range of HR. One of these instruments, the MIC, employed an upper bandlimit of 15 Hz for dZ/dt and 60 Hz for ΔZ. The other instrument, the UM impedance cardiograph, used an upper bandlimit of 50 Hz for dZ/dt and 120 Hz for ΔZ. An additional comparison was performed to determine whether digitally computing the dZ/dt from the ΔZ signal, using a digital differentiator with a 50 Hz corner frequency, would yield different amplitude and event location measurements from the values derived from the analog dZ/dt signals.

In general, the results showed that the 15 Hz low pass filter used in the MIC substantially attenuated the dZ/dt amplitude and SV measurements relative to the other analog dZ/dt and digitally computed measurements. This effect occurred both at slower HRs attenuating dZ/dt_{max} and SV by about 13% and increased at faster HRs attenuating dZ/dt_{max} and SV by about 26%. The differential influence with increasing HR of impedance cardiograph signal fidelity may, in part, explain the findings of a recent validity study, which compared SV estimates simultaneously derived from impedance cardiography and nuclear ventriculography during exercise (Wilson et al., 1989). It was found that at higher exercise workloads and consequently higher HRs impedance-derived SV values underestimated the comparison method. Moreover, increasingly poorer correlations between methods for SV were obtained with increasing workload. Thus instances of poor validity of ICG-derived values in some individuals with rapid HRs and during challenge conditions that induce cardiac activation (cf. Handelsman, 1989) may largely reflect the signal fidelity of the front-end impedance cardiograph amplifier.

The shape and temporal location of the events within the signal were also affected by the upper bandlimit settings as can be seen clearly in Fig. 5. Less resolution and greater flattening of the waveform events (B and X waves) and broadening of the dZ/dt peak occurs when the corner frequency is set at 15 Hz than with the other low-pass filter settings. The impact of the signal fidelity on the temporal location of the events can be seen in the systolic time interval findings. Since the PEP, QZ and QX intervals are all timed from the Q wave, differences in the systolic time interval durations would reflect a differential influence of the four measurement methods on the three ICG events. From these results the MIC-15 Hz instrument consistently produced the longest intervals in each of the HR target ranges. The other analog

signal, from the UM-50 Hz instrument, produced similar PEP but shorter QZ and QX intervals than the MIC-15 Hz instrument. The two other methods using the digitally differentiated ΔZ signals produced similar and shorter intervals than the analog methods. Since both of the analog methods produced signal delays it might be suggested that the 15 Hz and 50 Hz low-pass filters of the analog instruments distorted the relevant ICG events to the extent that local minima (for B and X waves) and maxima (for the Z-peak) occurred at later points in time thereby producing more prolonged systolic time intervals. This may be the case for the MIC-15 Hz effect but the UM-50 Hz amplifier may not be distorting the ICG events, because in analog differentiators there is an inherent signal delay due to the response time of the circuit components that is not present in the digital differentiator used in this study. Therefore, the difference between the UM-50 Hz and the digital methods in systolic time interval duration (about 8–9 ms) most probably reflects this inherent difference. This hypothesis is supported by the fact that there were no differences between the UM-50 Hz and the two digital methods in LVET, whereas the MIC-15 Hz LVET was more prolonged. Indeed, the difference between the other methods and the MIC-15 Hz method in LVET can be accounted for by the differential influence of the latter method on the locations of the B and X. That is, the delay in X minimum location was 6.3 ms greater than the delay in the B point location, which is exactly the observed difference in LVET between the MIC-15 Hz and the other methods.

These findings indicate that, when an upper bandlimit less than 50 Hz is used to filter the ICG signal a systematic underestimation of dZ/dt_{max} and an overestimation of the systolic time intervals occurs. The underestimation of dZ/dt_{max} becomes greater with increasing heart rate whereas the differences in systolic time interval measurement are not dependent on cardiac activational level. However, it should be noted that the effect on the systolic time intervals was not uniform. If it can be assumed that the inherent delay in the analog differentiator is the delay present in the UM-50 Hz signal (i.e. about 9 msec) then it can be concluded that the delay induced by the MIC-15 Hz in the QB interval, which was about 9.4 ms, was nothing more than this inherent electro-mechanical delay and not due to B point distortion. It then follows that the delay produced by the MIC-15 Hz filter in the X minimum location was about 7.4 ms and the delay in the Z peak was about 21.7 ms. Since it appears that the 15 Hz low-pass filter affected only the Z-peak and X waves event locations, then it may be concluded that these waveforms have spectral components in the higher frequency bands, which have rendered them susceptible to low-pass filtering distortion. The implication of this finding is that estimates of myocardial contractility such as the Heather index (Heather, 1969) or the acceleration index (Kizakevich et al., 1989), which involve the detection of the dZ/dt peak location, will be more greatly

affected than measures involving the X minimum detection for calculation of LVET or electrical mechanical systole, for example, although each of these estimates will be influenced to some extent.

There are serious implications of these findings for studies using impedance cardiographs with bandlimits less than 50 Hz. For example, psychophysiological studies of cardiovascular reactivity, which typically compare the cardiac activational response to a behavioral challenge with pretask resting levels may yield results that are confounded between groups and within individuals simply because the differential influence of the low-pass filter on SV is dependent on HR. That is, subjects with faster HRs will tend to have diminished SVs and less distinct differences will be produced between more and less reactive subjects. Therefore, the contention that it is sufficiently valid to use impedance cardiography to derive change-score information even though absolute levels may not be valid (cf. Sherwood et al., 1990) may be an untenable position during some instances in light of this evidence, which shows a differential loss of ICG amplitude information from resting to non-steady state conditions.

The two instruments with similar 50 Hz corner frequencies (i.e. the UM-50 Hz and the MIC-60 Hz) produced similar amplitudes of the dZ/dt_{max} and similar SV values. However, the digitally computed dZ/dt_{max} derived using the UM-120 Hz instrument, which collected the ΔZ signal with a low-pass filter of 120 Hz but contained a 50 Hz corner frequency within the digital differentiator resulted in about a 6% increase over these values at each of the HR levels. This shows that, as would be expected, the low order analog filters—60 Hz low pass filter for ΔZ and 50 Hz differentiators—due to their non-ideal characteristics in the vicinity of the corner frequencies, attenuate high frequency components of the ICG signal, which are present regardless of cardiac activation level. To pass these frequencies, the analog instrument would require bandwidths larger than 50 Hz, which in turn would decrease the signal-to-noise ratio and undesirably retain more signal artifacts. Although all three instruments with the extended bandwidth resulted in greater SV and dZ/dt_{max} values than the 15 Hz instrument, the question of whether these greater SV values are more accurate requires validational comparison. If the method using digital differentiation of ΔZ is as valid or proves more valid than the analog method then the digital method would be recommended because the estimates of systolic time intervals will not include a signal delay.

When using the digital method, the issue of ΔZ balancing is a factor in measurement accuracy. The sample and hold balancing method used in most impedance cardiographs is highly susceptible to motion artifact and resulted in about a 30% loss of cardiac cycles during exercise. However, the use of the real-time automatic balancing circuit, which in this study completely removed this source of signal distortion, improves the viability of the digital method

for use in behavioral challenges that require movement. In addition, by virtue of setting the ICG amplifier for transducing ΔZ at corner frequencies greater than 50 Hz, the digital method also permits recording from human or animal subjects whose HRs are greater than 150 bpm. Since all biological signals contain more or less unremovable variation (i.e. noise) that have spectral components overlapping with those of the signal, it is impossible to select a corner frequency such that the output waveform includes only the spectral components of the signal. Appropriate off-line digital filtering techniques can be used in these situations to separate signal from contaminated waveforms. However, as shown in this study, an amplifier with an adequate bandwidth is necessary to preserve as many signal components as possible to improve the validity of the ICG signal and the reliability of event location.

Acknowledgments

This work was supported by National, Heart, Lung and Blood Institute of the National Institutes of Health grants, HL31648 and HL36588.

References

Anderson, J.S., Cobbold, R.S.C., & Johnston, K.W. (1981). Dual-channel self-balancing impedance plethysmograph for vascular studies. *Medical and Biomedical Engineering and Computing, 19*, 157–164.

Appel, P.L., Kram, H.B., MacKabee, J., Fleming, A.W., & Shoemaker, W.C. (1986). Comparison of measurements of cardiac output by bioimpedance and thermodilution in severely ill surgical patients. *Critical Care Medicine, 14*, 933–935.

Bernstein, D.P. (1986). Continuous noninvasive real-time monitoring of stroke volume and cardiac output by thoracic electrical bioimpedance. *Critical Care Medicine, 14*, 898–901.

Fuller, H., Raskob, G., ter Keurs, H., & Hull, R. (1989). The current status and future directions of impedance cardiography in ICU. *Annals of Biomedical Engineering, 17*, 483–494.

Geddes, L.A., & Baker, L.E. (1989). Principles of applied biomedical instrumentation. (3rd Ed.). New York: Wiley.

Goldstein, D.S., Cannon, R.O., Zimlichman, R., & Keiser, H.R. (1986). Clinical evaluation of impedance cardiography. *Clinical Physiology, 6*, 235–251.

Handelsman, H. (1989). Public Health Service Assessment: Cardiac output by electrical bioimpedance, 1989. Rockville, MD: DHHS Publication No. (PHS) 89-3441, pp. 1–5.

Heather, L.W. (1969). A comparison of cardiac output values by the impedance cardiograph and dye dilution techniques in cardiac patients. In W.G. Kubicek, D.A. Witsoe & R.P. Patterson (Eds.), *Development and evaluation of an impedance cardiographic system to measure cardiac output and other cardiac parameters*. Houston, TX: NASA Publication CR 101965, pp. 247–258.

Hurwitz, B.E., Shyu, L-Y., Reddy, S.P., Schneiderman, N., & Nagel, J.H. (1990). Coherent ensemble averaging techniques for impedance cardiography. In H.T. Nagle and J.N. Brown (Eds.), *Computer-based medical systems*. Washington, DC: IEEE Computer Society Press, pp. 228–235.

Kizakevich, P.N., Teague, S.M., Jochem, W.J., Nissman, D.B., Niclou, R., & Sharma, M.K. (1989). Detection of ischemic response during treadmill exercise by computer-aided impedance cardiography. *Proceedings of the 2nd annual IEEE symposium on computer-based medical systems*. New York: IEEE catalog 89CH2755-7, pp. 10–15.

Kubicek, W.G., Witsoe, D.A., Patterson, R.P., & From, A.H.L. (1969). *Development and evaluation of an impedance cardiographic system to measure cardiac output and other cardiac parameters* (NASA-CR-101965). Houston: National Aeronautics and Space Administration.

Kubicek, W.G., Karnegis, J.N., Patterson, R.P., Witsoe, D.A., Mattson, R.H. (1974). The Minnesota impedance cardiograph—theory and applications. *Biomedical Engineering, 9*, 410–416.

Lu, C-C. (1991). *Design of a real-time self-balancing impedance plethysmograph*. Unpublished master's thesis. University of Miami, Coral Gables, FL.

Miller, J.C. & Horvath, S.M. (1978). Impedance cardiography. *Psychophysiology, 15*, 80–91.

Sherwood, A., Allen, M.T., Fahrenberg, J., Kelsey, R.M., Lovallo, W.R., & van Doornen, L.J.P. (1990). Methodological guidelines for impedance cardiography. *Psychophysiology, 27*, 1–23.

Shyu, L-Y. (1992). *Systematic investigation of event detection, hardware, and models for impedance cardiography*. Unpublished Doctoral dissertation, University of Miami, Coral Gables, FL.

Wilson, M.F., Sung, B.H., Pincomb, G.A., & Lovallo, W.R. (1989). Simultaneous measurement of stroke volume by impedance cardiography and nuclear ventriculography: comparisons at rest and exercise. *Annals of Biomedical Engineering, 17*, 475–482.